Journal of Cosmology and Astroparticle Physics
An IOP and SISSA journal

Received: *March 21, 2024*
Revised: *July 30, 2024*
Accepted: *December 9, 2024*
Published: *January 23, 2025*

Spacetime surgery for black hole fireworks

Wei-Chen Lin[a,b] **Dong-han Yeom**[a,d,e,f] **and Dejan Stojkovic**[c]

[a]*Center for Cosmological Constant Problem, Extreme Physics Institute, Pusan National University, Busan 46241, Republic of Korea*
[b]*Department of Physics, Pusan National University, Busan 46241, Republic of Korea*
[c]*HEPCOS, Department of Physics, SUNY at Buffalo, Buffalo, NY 14260, U.S.A.*
[d]*Department of Physics Education, Pusan National University, Busan 46241, Republic of Korea*
[e]*Research Center for Dielectric and Advanced Matter Physics, Pusan National University, Busan 46241, Republic of Korea*
[f]*Leung Center for Cosmology and Particle Astrophysics, National Taiwan University, Taipei 10617, Taiwan*

E-mail: archennlin@gmail.com, innocent.yeom@gmail.com, ds77@buffalo.edu

Abstract: We construct an explicit model for the black hole to white hole transition (known as the black hole fireworks scenario) using the cut-and-paste technique. We model a black hole collapse using the evolution of a time-like shell in the background of the loop quantum gravity inspired metric and then the space-like shell analysis to construct the firework geometry. Our simple and well-defined analysis removes some subtle issues that were present in the previous literature [1] and makes the examination of the junction conditions easier. We further point out that the infalling and asymptotic observers, both in ours and the original scenario in ref. [1], encounter quite different physics. While the proper time of the bounce for an infalling observer can be determined without ambiguity, the bouncing time interval for the asymptotic observer can be chosen arbitrarily by changing how one cuts and pastes the spacetimes outside the event horizons. It is puzzling that the proper time of a distant (rather than infalling) observer is subject to randomness since the infalling observer is supposed to experience a stronger quantum gravity effect. This result might suggest that a black hole firework scenario does not allow for the existence of an effectively classical spacetime inside the horizon. The main message is therefore that even if we strictly follow the thin shell formalism to cut and paste spacetimes, this does not guarantee that the resulting spacetime offers a physically reasonable background.

Keywords: Gravastars, quantum black holes

ArXiv ePrint: 2310.15508

https://doi.org/10.1088/1475-7516/2025/01/098

JCAP01(2025)098

Contents

1 Introduction

The issue of formation and evaporation of a black hole is very important for understanding the nature of quantum gravity. In particular, this issue is related to the information loss problem of an evaporating black hole [2]. Is there a unitary theory of quantum gravity that explains the unitary evolution of evaporating black holes? If there is, is this theory consistent with the semi-classical description [3]? Will the classical singularity survive in the regime where quantum gravitational effects are dominant [4, 5]?

It is clear that understanding the fate of the singularity is very important to obtain the complete answer to the black hole evaporation and the information loss problem. Intuitively, we may classify two ways. First, we may address this problem *by introducing a wave function*, i.e., by solving the Wheeler-DeWitt equation [6]. In this approach, we need to solve the Wheeler-DeWitt equation (or some version of it) and interpret the solution in the classical background, which is sometimes a subtle problem [7–10]; for an attempt to model quantum radiation from quantum background, see [11]. Second, we may remove the singularity *by introducing an effective matter* [12–16]. As a result, one could extend the effectively classical spacetime beyond the singularity. However, we need to justify the ad hoc introduced matter from the first principles, which is usually a difficult task.

Interestingly, an approach coming from the loop quantum gravity provides a method that is in between these two ways. In that approach, one first needs to solve the Wheeler-DeWitt equation to obtain the physical quantum state of the singularity. Usually, it is not easy to solve the Wheeler-DeWitt equation directly. However, one may reasonably expect an effective modification of the Hamiltonian which includes loop quantum gravitational effects [17]. With this modified Hamiltonian, one can solve a set of semi-classical equations and obtain a spacetime that includes loop quantum gravitational effects, e.g., resolution of the singularity.

A typical solution in the framework of the loop quantum gravity includes *bouncing* of the collapsing object [18, 19] (see also [20, 21]). Bouncing inside the horizon is not a very surprising scenario, except for some technical issues [22]. However, in reality, this is not easy to generalize to global spacetimes in an evaporating background. In some cases, inconsistencies may arise [23]. In an evaporating background, the bouncing spacetimes have to consistently connect not only inside but also outside the horizon [24]. A similar spacetime structure happens in the more exotic proposal introduced in the Haggard-Rovelli model [25], where the quantum gravitational effects can accumulate outside the apparent horizon and modify the metric beyond it. The resulting spacetime might be realized by cutting and pasting spacetimes both inside and outside the apparent horizon. In [1], Han, Rovelli, and Soltani extend this idea to the black hole solution with quantum gravity modification, which gives a bouncing model that has two horizons. The scenario proposed in [1, 25] is also known as the *black hole fireworks*.

In this paper, we investigate this idea in the model in ref. [1], in which the spacetime contains both the inner and outer horizons and the proposed bouncing effect changes the topology of the spacetime to have only one asymptotic infinity. To simplify the discussion, we consider a time-like shell that describes a collapsing star interior and the dynamical formation of a black hole. In addition, we offer a simplified cut-and-paste procedure to accommodate a similar bouncing spacetime and to cover both the outer and inner apparent horizons. This simplified approach is technically well-defined and makes the examination of junction conditions more straightforward.

However, apart from the validity of the spacetime from the justification of junction conditions, in the resulting spacetimes constructed in both ref. [1] and this article, there exists a more fundamental issue. We notice this issue by tracking the trajectories of different observers theoretically existing in these spacetimes. The bouncing time interval measured for the distant observer can be chosen arbitrarily since it is determined mathematically by how one cuts and pastes the spacetimes outside the event horizons. In contrast, for an infalling observer who travels through the black and white hole apparent horizons and then out, the duration of the bounce measured by his proper time can be determined with little ambiguity. The unexpected outcome suggests that there may not be a semi-classical spacetime within the inner event horizon in the black hole fireworks scenario. Therefore, simply employing the cut-and-paste procedure is not adequate to describe the black hole fireworks, even if assuming that tunneling outside the horizon is possible.

This paper is organized as follows. In section 2, we consider a collapsing time-like shell and the dynamical process of black hole formation based on the black hole bouncing model of ref. [1]. We briefly review the procedure and the resulting spacetime given by ref. [1] and then offer a simplified procedure to construct a similar bouncing model, in which the junction conditions are easier to examine. In section 3, we discuss the bouncing time scales from the black hole and white hole phases defined by two types of observers allowed by the setting. We show that the proper time of the infalling type of observer is not affected much

JCAP01(2025)098

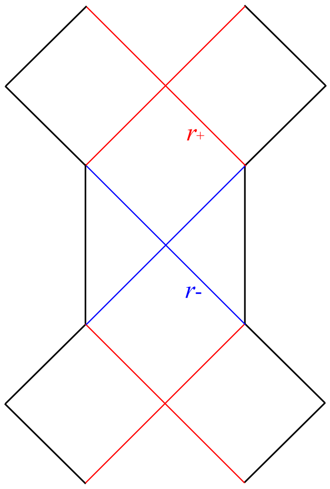

Figure 1. The Penrose diagram of the model in eq. (2.1). The solution has two horizons, $r_\pm$, and the time-like center.

by the cut-and-paste procedure, which is very different from the bouncing time defined by any distant observer. We conclude that this fact challenges the existence of an effectively classical spacetime inside the horizons for the black-hole-firework scenario. Finally, in section 4, we summarize our results and discuss possible future research.

2 The cut-and-paste procedure for the black hole firework

In this section, we utilize the gravitational collapse of a time-like thin-shell to revisit the cut-and-paste procedure introduced in ref. [1], in which a black hole model with a quantum-corrected center proportional to $1/r^4$ is considered. We next reproduce a similar resulting spacetime by considering a simplified cut-and-paste procedure consisting of two space-like hypersurfaces. Both the collapsing thin-shell and the space-like cuts modeling the black-to-white hole tunneling follow the formalism of the Israel junction conditions, and the construction is shown explicitly. We also briefly discuss the difference between the two different cut-and-paste procedures.

2.1 Time-like thin-shells and gravitational collapses

We consider the black hole model defined in [1], which has a quantum-corrected center. The metric is

$$ds^2 = -f(r)dt^2 + \frac{1}{f(r)}dr^2 + r^2 d\Omega^2, \tag{2.1}$$

with

$$f(r) = 1 - \frac{2M}{r} + \frac{AM^2}{r^4}, \tag{2.2}$$

where M is the black hole mass, while A is a constant. Generically, this geometry has two horizons, labeled with $r_\pm$, with a time-like center (figure 1). We note here that the bounce in this model is driven by the AM^2/r^4 term in eq. (2.2). This term dominates only at small values of r, and provides a repulsive gravity. Thus, directly from this form, we expect an

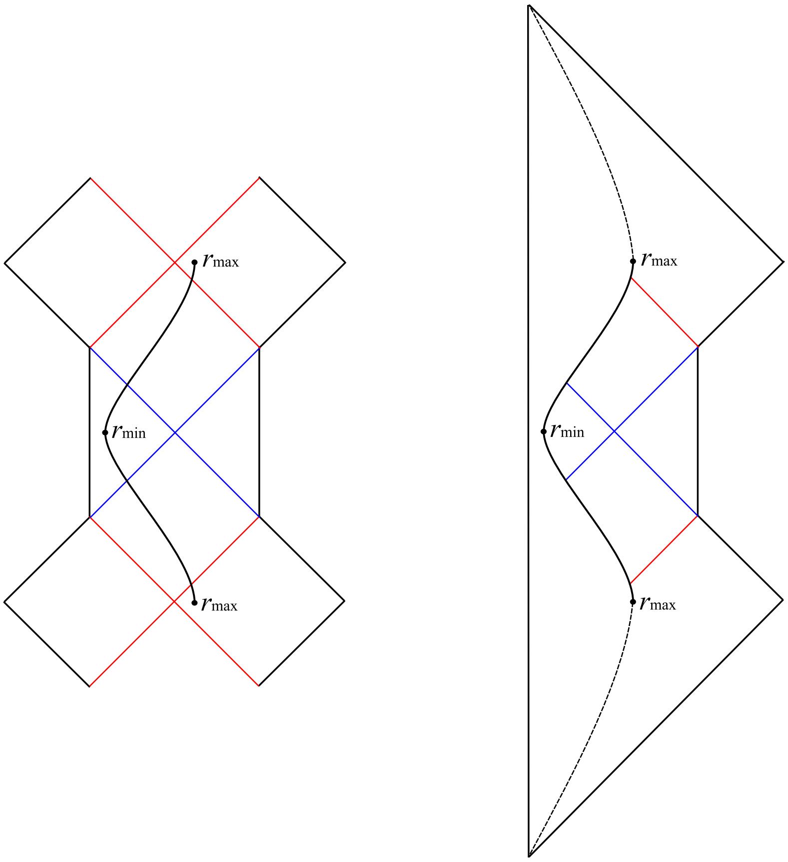

Figure 2. Left: the Penrose diagram of the black hole solution, where the red lines are outer horizons and the blue lines are inner horizons. There exists a time-like shell solution that is oscillating between $r_{\rm min} \leq r \leq r_{\rm max}$, where $r_{\rm max}$ is outside the outer horizon and $r_{\rm min}$ is inside the inner horizon. Right: inside the shell, the geometry is Minkowski. This diagram represents the resulting spacetime of the black hole formation.

oscillating behavior. At large values of r, the attractive term, $2M/r$, dominates and drives the collapse. At some minimal value of r, the repulsive term causes bounce and pushes the collapsing object out to larger values of r where the attractive term again dominates and the cycle starts again.

Now, we review the thin-shell approximation of a collapsing time-like thin-shell under this metric. The metric outside and inside the shell is

$$ds_{\pm}^2 = -f_{\pm}(r)dt^2 + \frac{1}{f_{\pm}(r)}dr^2 + r^2 d\Omega^2, \tag{2.3}$$

where $+$ and $-$ stand for outside and inside the shell, respectively. The metric of the time-like shell is

$$ds_{\rm shell}^2 = -d\tau^2 + r^2(\tau)d\Omega^2. \tag{2.4}$$

Here, we assume $f_+ = f(r)$ and $f_- = 1$.

After imposing the junction equation [26], we obtain

$$\epsilon_- \sqrt{\dot{r}^2 + f_-} - \epsilon_+ \sqrt{\dot{r}^2 + f_+} = 4\pi r \sigma(r), \tag{2.5}$$

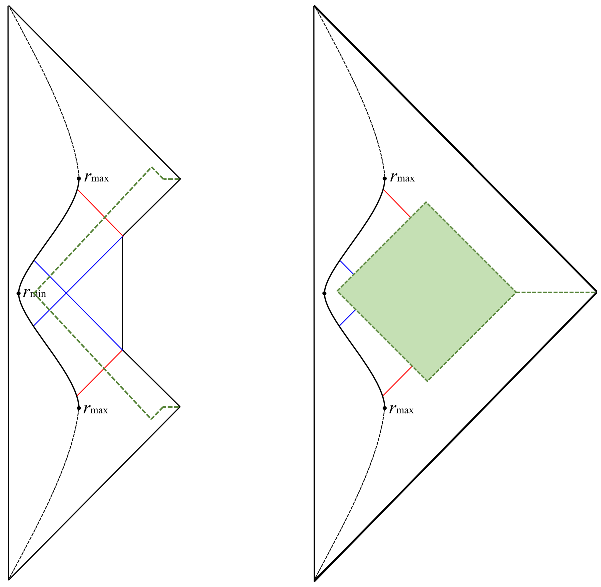

Figure 3. Left: the green dashed line indicates the single complex cut introduced in ref. [1], which consists of two constant-t spacelike hypersurfaces and four null hypersurfaces. Right: the resulting spacetime is constructed by discarding the right piece to the cut and then pasting the two constant-t spacelike hypersurfaces together. This procedure leaves an empty area (light green) whose boundary is given by the four null hypersurfaces that are parts of the complex cut, and the metric of this area is determined by the continuity condition. Notice that pasting two constant-t spacelike hypersurfaces does not require the existence of any thin-shell, so the violation of the NEC is limited to the light green region.

where $\sigma(r)$ is the tension of the shell, and $\epsilon_\pm = \pm 1$ are the signs of the extrinsic curvatures. Here, extrinsic curvatures $\beta_\pm$ are

$$\beta_\pm \equiv \frac{f_- - f_+ \mp 16\pi^2\sigma^2 r^2}{8\pi\sigma r} = \epsilon_\pm \sqrt{\dot{r}^2 + f_\pm}. \tag{2.6}$$

Note that if $\epsilon_\pm = +1$, r increases along the outward normal direction, while if $\epsilon_\pm = -1$, r decreases along the outward normal direction. Therefore, we have to assume $\epsilon_\pm = 1$.

After simple computations, we obtain the equation:

$$\dot{r}^2 + V_{\text{eff}}(r) = 0, \tag{2.7}$$

where

$$V_{\text{eff}}(r) = f_+ - \frac{\left(f_- - f_+ - 16\pi^2\sigma^2 r^2\right)^2}{64\pi^2\sigma^2 r^2}. \tag{2.8}$$

Here, we interpret that $V_{\text{eff}} < 0$ corresponds to the region where classical trajectories are allowed. To form a black hole, one can set $\sigma = \sigma_0$, and assume $\lambda/\sigma = -1$, where λ is the pressure of the shell. For example, a scalar field can satisfy such a condition [31]. In appendix A.1, we give the numerical results of some time-like thin-shell examples.

2.2 The construction of the black hole firework geometry introduced in ref. [1]

After constructing the Penrose diagram of a collapsing thin-shell under the metric eq. (2.2), we now briefly review the cut-and-paste procedure introduced in ref. [1]. Here we only focus

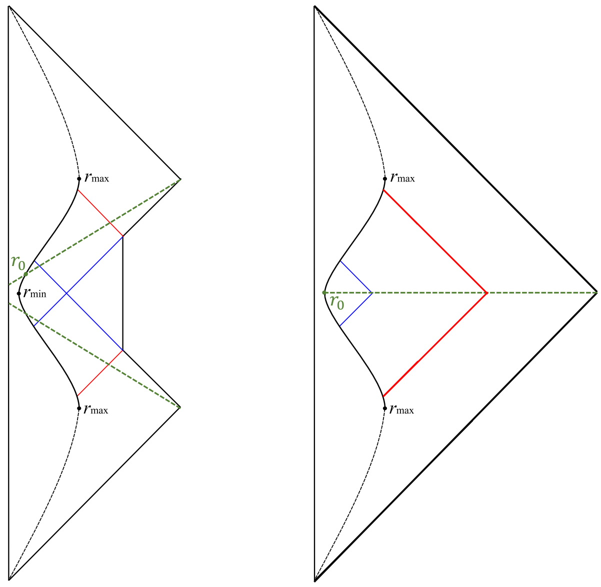

Figure 4. Left: the two green dashed lines indicate the simplified cutting procedure that we adopt. Right: the causal structure resulted from pasting two space-like slices.

on the general features of the procedure and of the resulting spacetime, which are sufficient for the discussions later. For more details, we refer the reader to the original paper.

In ref. [1], the authors introduce a single but complex cutting of spacetime which is composed of two constant-t hypersurfaces connecting to different spatial infinities and four different null hypersurfaces as shown in figure 3 (left). Then, by keeping only the side containing the collapsing thin-shell, the pasting procedure is simply given by identifying the two constant-t hypersurfaces to be the same as shown in figure 3 (right). This procedure leaves an empty region (the light green part in the figure), in which the metric is not given by eq. (2.2) but is determined by the continuity of the metric at the boundary. Notice that pasting constant-t hypersurfaces does not require the existence of any thin-shell, and thus, the possible violation of the null energy condition (NEC) is limited to the light green area. The resulting spacetime, which we will refer to as the **HRS model** in the rest of this work, is then semi-classical everywhere and has only one asymptotic infinity. Lastly, the complex cutting procedure implemented here creates corners outside the outer event horizon, so the corner conditions must be satisfied to avoid the conical singularity [32]. To avoid this complexity, in the following subsection, we will consider a simplified cut-and-paste procedure to reproduce a similar bouncing model with the same global structure. This simplified procedure has the advantage that the junction conditions are more straightforward to examine.

2.3 The simplified construction of the black hole firework geometry

It is not difficult to observe that to construct a Penrose diagram with the same global structure given in figure 3, the simplest way is to cut and paste two general space-like hypersurfaces from two different asymptotic spatial infinities, as shown in figure 4. We call the resulting spacetime the **minimal model**. Notice that we choose that the time-like and space-like slices intersect at $r = r_0$, deep inside the inner event horizon. One can also choose to have the two space-like slices intersect each other inside the inner horizon like the cut shown in figure 3, thus creating a corner. In either case, the intersecting point or the corner is deep inside the inner horizon, where a complete description of this intersection perhaps belongs to the regime of quantum gravity. Thus, we neglect the possible complications in this regime and simply consider the junction conditions of a general space-like shell given in figure 4 (right). Since the formalism of the thin-shell approximation is similar to the case of a time-like shell we have discussed in section 2.1, we leave the derivation and numerical examples in appendix A.2.

Though both resulting spacetimes have the same global structure, some differences exist due to the different cut-and-paste procedures used to model the bounce. Here, we make some remarks on the qualitative differences and some special features shared by both that will be important to the next section:

- 1. In the minimal model, the violation of the NEC happens along the shell and reaches infinity. Although the effect can approach zero asymptotically, violation of NEC far away from the black hole is expected. In the HRS model, the possible violation of the NEC can be limited to the light green region in figure 3 (right).[1]

- 2. In the minimal model, there is no corner or intersection of thin-shells outside the event horizon. However, corners exist outside the event horizons in the HRS model. There is no guarantee that the corner conditions can be satisfied, for which the violation leads to the conical singularity.

- 3. In both of the models, one can choose having either a corner (formed by two null hypersurfaces in the HRS model or by two spacelike hypersurfaces in the minimal model) or intersections between the collapsing shell and the null/space-like hypersurfaces inside the inner event horizon.

- 4. Both of the models have only one asymptotic infinity, which is topologically different from the original classical spacetime given by the metric eq. (2.2).

Although there might be some interest in determining the exact range of the violation of the NEC and the corner conditions required in the HRS model, in the next section we focus on remark 4 to argue that the existence of a semi-classical spacetime inside the inner event horizon is improbable in both models by considering the bouncing time for different observers.

3 Bouncing time-scale for black hole firework scenarios

In this section, we discuss the bouncing time observed by different observers. We use the same assumption that the quantum gravity corrections should be small, i.e. $A \sim m_{Pl}^2 \ll M^2$. In this limit, the parameter A plays no role in the leading order estimate, and therefore, the mundane Schwarzschild solution is sufficient for this particular discussion.[2] We first re-derive the bouncing time for a distant observer at a fixed R as presented in ref. [1]. After that, we calculate the bouncing time measured by the observer who is comoving with the shell and then discuss the slicing dependence of the two different bouncing times in section 3.3.

[1]For the demonstration of the violation of NEC in the back-to-white hole bounce in different models, see refs. [27–30].

[2]Though, we comment on the possible relation between δ and A later in section 3.3.

JCAP01(2025)098

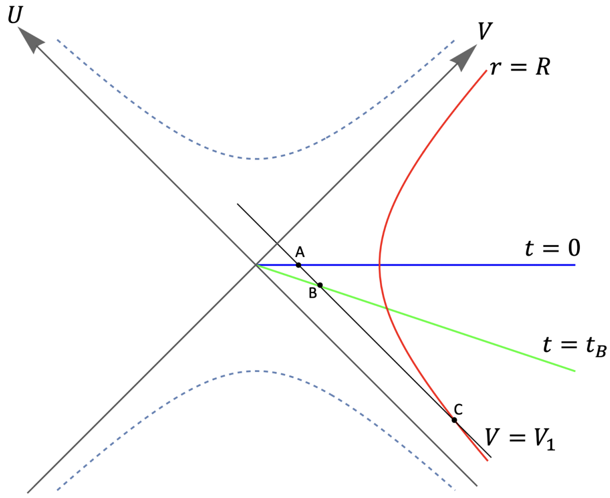

Figure 5. Bouncing time in the Schwarzschild metric. In ref. [1], the trajectory of $V = V_1$ is uniquely determined by the corresponding spacetime diagram therein. However, the bouncing time, defined by $\mathcal{T} \equiv -4M \ln \delta$ in ref. [1], is rooted from a geometric relation in the Schwarzschild spacetime, eq. (3.4). It means that the duration of bouncing time defined in this way is related to the arbitrary cutting of spacetime.

3.1 Bouncing time scale with the δ parameter

Outside the horizon, the black hole is well approximated by the Schwarzschild solution. Assuming the Schwarzschild solution, the double-null coordinates U and V satisfy

$$UV = \left(1 - \frac{r}{2M}\right) e^{r/2M} \tag{3.1}$$

and

$$\frac{U}{V} = -e^{-t/2M}, \tag{3.2}$$

in the region of interest (see figure 5). In figure 5, events A, B, and C are given by the intersections of a specific ingoing light ray $V = V_1$ with the constant-t hypersurfaces, $t = 0$ and $t = t_B$, and a constant-r trajectory $r = R$, respectively. Since t_B is an arbitrary constant, event A is just a special case with $t_B = 0$.

In terms of the Schwarzschild coordinate (t, r), the locations of B and C are given by $(t_B, 2M + \Delta)$ and (t_C, R), respectively. Using (3.1) and (3.2), one can show that the quantities Δ, t_B, and t_C satisfy the following relation

$$\frac{\left(\frac{R}{2M} - 1\right) e^{R/2M}}{\frac{\Delta}{2M} e^{(1+\Delta/2M)}} = e^{\tilde{T}/4M}, \tag{3.3}$$

where $\tilde{T} \equiv 2(t_B - t_C)$. Assuming $\Delta \ll 2M \ll R$, the above relation reduces to

$$\tilde{T} \approx 2R + 4M \ln R - 4M \ln \Delta. \tag{3.4}$$

By choosing $t_B = 0$, i.e. considering event A with location $(t, r) = (0, 2M + \delta)$, we obtain the relation given in ref. [1]

$$T \approx 2R + 4M \ln R - 4M \ln \delta, \tag{3.5}$$

where $T/2 \approx -t_C$. In ref. [1], the term independent of R on the r.h.s. of eq. (3.5) is defined to be the bouncing time of the black-to-white hole tunneling, $\mathcal{T} \equiv -4M \ln \delta$. However, here we see that it is a special case of eq. (3.4), when $t_B = 0$ is chosen. Since the metric (2.2) or its approximation, Schwarzschild metric, are both static, choosing $t_B = 0$ to cut and paste spacetime bears no special meaning. From the mathematical point of view, one can choose any other constant t_B-hypersurface to construct the resulting cut-and-pasted spacetime with different bouncing time given by the similar definition from eq. (3.4): $\mathcal{T} \equiv -4M \ln \Delta$. Then, this arbitrariness on the choice of the constant t_B-hypersurface to perform the cut-and-paste procedure gives the arbitrariness of the bouncing time defined in this way. Later, we will discuss the issue of this arbitrariness from the physical point of view. Before ending this subsection, we would like to point out that eq. (3.4) has a simple physical interpretation by itself. A distant observer shoots a ray of light radially into the black hole from event C. After $\tilde{T}/2$ of this observer's proper time elapsed, the observer would think the light ray is Δ away from the event horizon.

3.2 Bouncing time for the comoving observer

Apart from the asymptotic observer whose coordinate system is incomplete, there is another observer who is perhaps more relevant to the bouncing process. This is an observer comoving with the collapsing shell. Thus, a more appropriate physical time scale can be calculated using the proper time of the observer that crosses the event horizon.[3] One can easily evaluate the proper time of the time-like shell that transitions from the black hole to the white hole phase as

$$\tau = 2 \left| \int_R^{r_{\min}} \frac{dr}{\sqrt{-V(r)}} \right|. \tag{3.6}$$

Here we use a collapsing shell of (pressureless) dust as a demonstration. In this case, the rest mass of the dust α is conserved and is given by $\alpha = 4\pi r^2 \sigma = const.$, where σ is the energy density of the shell. From the Israel junction conditions, we obtain

$$M = \alpha\sqrt{1 + \dot{r}^2} - \frac{\alpha^2}{2r}, \tag{3.7}$$

where the overdot is the derivative with respect to the proper time along the timelike trajectory of the infalling shell. From this, one can compute the proper time elapsed along the shell trajectory for one complete cycle as follows

$$\tau = 2 \left| \int_{R_{\max}}^{r_{\min}} \frac{dr}{\sqrt{\left(\frac{M}{\alpha} + \frac{\alpha}{2r}\right)^2 - 1}} \right|. \tag{3.8}$$

To have $R_{\max}$ finite, i.e. the shell is bounded, we must have $\alpha > M$, for which $R_{\max} = \frac{\alpha^2}{2(\alpha - M)}$. In this case, the above integral is given by

$$\tau = 2\sqrt{\frac{1}{1 - \frac{M^2}{\alpha^2}}} \left(\frac{1}{2} C \tan^{-1} \left(\frac{2r - C}{2\sqrt{Cr + B - r^2}} \right) - \sqrt{Cr + B - r^2} \right) \Bigg|_{r_{\min}}^{R_{\max}}, \tag{3.9}$$

[3] Notice that here we consider the assumption that spacetime is effectively classical and the metric (2.2) is valid even when r is small, $r \ll 2M$. Under this assumption, this comoving observer can be defined in principle.

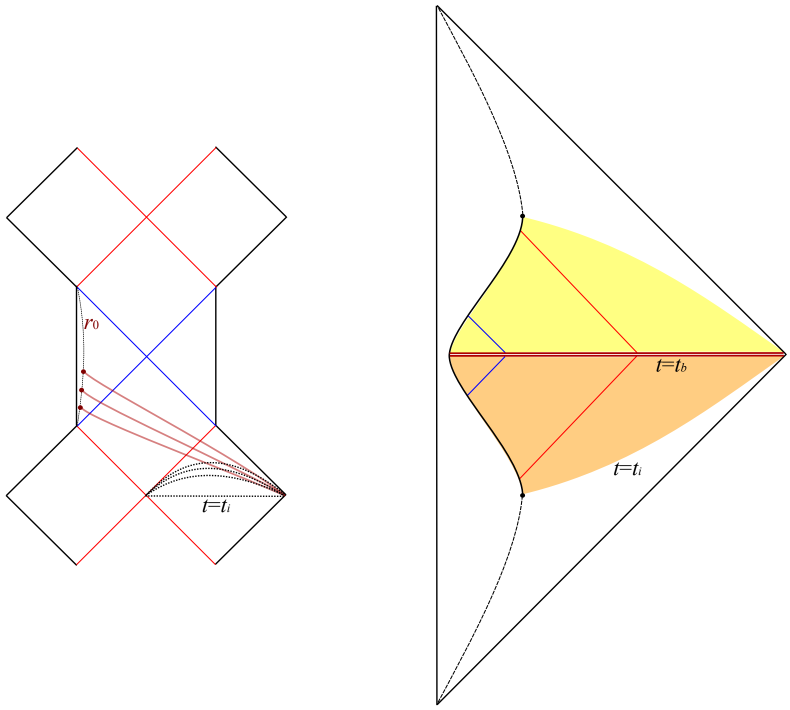

Figure 6. Left: due to the time-translation symmetry, there can be several equivalent spacelike slices (red curves) that have a different coordinate time at infinity. Black dotted curves correspond to constant t hypersurfaces. Right: the bouncing time is the difference between $t = t_i$ and $t = t_b$, where t_b is arbitrary.

where $C = \frac{M}{1-\frac{M^2}{\alpha^2}}$ and $B = \frac{\alpha^2}{4\left(1-\frac{M^2}{\alpha^2}\right)}$. If we further consider large $R_{\text{max}} \gg M$, based on the relation for R_{max}, we also have $\alpha \sim 2R_{\text{max}}$. Thus, the above integration is approximately given by

$$\tau \sim 2\left|\int_{R_{\text{max}}}^{r_{\text{min}}} \frac{dr}{\sqrt{\left(\frac{\alpha}{2r}\right)^2 - 1}}\right| \sim 2\left|\int_{R_{\text{max}}}^{r_{\text{min}}} \frac{dr}{\sqrt{\left(\frac{R_{\text{max}}}{r}\right)^2 - 1}}\right| = 2\sqrt{R_{\text{max}}^2 - r_{\text{min}}^2}. \tag{3.10}$$

In this limit, the bouncing time is mostly determined by R_{max}, while the exact value of r_{min} is not that important. This is physically reasonable since in this limit, the shell's velocity relative to the center of the black hole is high when r is small. If we include the quantum gravity modification, i.e. using the metric in eq. (2.2) instead of the Schwarzschild solution, the shell will be repelled at some minimal radius due to the extra repulsive term AM^2/r^4. Thus, we have to set the r_{min} to be the bouncing point inside the horizon, which is determined by the three parameters $\{\alpha, M, A\}$. However, due to the smallness of AM^2, the bouncing point must be deep inside the event horizon, and the modifications to eqs. (3.9) and (3.10) are small.

3.3 Is an effective classical spacetime inside the horizons consistent with a tunneling picture?

We now analyze the coordinate time difference between two slices (figure 6) in our construction. Due to the *time-translation symmetry*, one can choose an arbitrary coordinate time (at infinity)

JCAP01(2025)098

for the space-like hypersurface (left of figure 6). This means that the time difference between the $t = t_i$ (that can be chosen in the sufficient past) and $t = t_b$ (the bouncing time inside the horizon) is arbitrary in this setup (right of figure 6), which is similar to the setting in ref. [1]. According to the discussion in section 3.1, one may find a corresponding δ parameter to denote the $t = t_b$ hypersurface. As already mentioned in ref. [1], the bouncing time for the distant observer is determined by how one cuts and pastes the spacetime outside the event horizon. The same argument is valid for the spacelike slicing considered in our case (see figure 6).

On the other hand, the bouncing time measured by the comoving observer discussed in section 3.2 is very different in this aspect. Based on the previous discussion, the contribution to the bouncing time around $r_{\min}$ is small, so even if we cut out a certain portion of the spacetime as in figure 4, the corresponding proper time is only mildly affected by the cut-and-paste procedure. Interestingly, this bouncing time can be unambiguously determined in the model considered in ref. [1] since the trajectory of the shell (or surface of the collapsing star) is intact by the designed cut (see figure 4 in ref. [1] or figure 3 in this article).[4] One can easily construct the scenario in which two observers (the comoving and the fixed-r one) begin their journeys at the same spacetime event when the shell is at some $R_{\max}$. After the whole period of the bounce, in the absence of any dissipation (as the assumption made in refs. [25] and [1]), the two observers meet each other again at the next $r = R_{\max}$. Without a doubt, the two observers experience different durations of proper time. One might think it is nothing but a generalization of the *twin paradox* result in Minkowski spacetime to a curved spacetime. However, the subtle issue here is that it is the distant observer's proper time subjected to arbitrariness instead of the proper time of the comoving observer who enters the regime where the quantum gravity effect is generally expected to be more dominant. From the mathematical construction discussed previously, we can see that it is due to the arbitrariness of choosing the cut-and-pasted hypersurface $t = t_b$ to obtain the resulting spacetime with a single asymptotic region, i.e. single past and future null infinity.

One might argue that the arbitrariness could be removed once we have the correct theory of quantum gravity. This is, in fact, argued by the authors of ref. [1]: "*A quantum theory of gravity must provide the probability distribution of $\mathcal{T}$ as a function of m. In the classical limit, $\mathcal{T} \to \infty$ and black holes are eternal.*" However, one should notice that the arbitrariness cannot be removed entirely from this physical point of view. In this scenario, the black-to-white hole bounce is due to a quantum tunneling effect, which is intrinsically subjected to the randomness of the probability distribution as pointed out by the authors of ref. [1]. Then, the issue still exists. That is, in the resulting spacetime, the proper time experienced by the infalling observer can be determined unambiguously, even in the quantum tunneling scenario. The question is then: "Is an effective classical spacetime inside the horizons still valid for such a tunneling picture?" If we forfeit the existence of semi-classical spacetime, at least, inside the inner apparent horizon, then an infalling observer following a classical trajectory into the black hole cannot be defined, and the conundrum is resolved.

[4] Nevertheless, it is a matter of choice as remark 3 we have mentioned in section 2.3.

Now, let us further consider the semi-classical description of tunneling by considering the following thought experiment. We start with two maximally entangled particles:

$$|\psi\rangle = \frac{1}{\sqrt{N}} \sum_i |i\rangle_{\rm in} |i\rangle_{\rm out}, \tag{3.11}$$

where N is the number of accessible states. One particle ($|i\rangle_{\rm in}$) falls into the black hole and is attached to the time-like shell, while the other particle ($|i\rangle_{\rm out}$) stays outside the black hole horizon. Whatever the time evolution of the quantum state $|\psi\rangle$ is, as long as the interactions of $|i\rangle_{\rm in}$ and $|i\rangle_{\rm out}$ are restricted by the local operations and classical communications, the entanglement entropy between two particles must be a constant.

However, we expect that the observer outside the horizon will experience quantum tunneling near the space-like shell, where the tunneling indicates a time evolution to a superposition of histories which depends on the tunneling time. Hence, the quantum state outside the horizon must be a superposition of different histories, i.e.,

$$|i\rangle_{\rm out} \to \sum_{j'} a^{(i)}_{j'} |j'\rangle_{\rm out}, \tag{3.12}$$

where the orthonormal basis $\{|i\rangle_{\rm out}\}$ and $\{|j'\rangle_{\rm out}\}$ are not equivalent in general.

In this context, let us define a semi-classical observer A which is inside the time-like shell. It is very reasonable to assume that the time evolution of the quantum state inside the shell follows a single classical history. On the other hand, let us define a semi-classical observer B which is outside the horizon. As long as the observer B is semi-classical, this observer will select a specific quantum state ($|k'\rangle_{\rm out}$) as an eigenstate such that

$$|i\rangle_{\rm out} \to \sum_{j'} a^{(i)}_{j'} |j'\rangle_{\rm out} \to a^{(i)}_{i'} |i'\rangle_{\rm out}, \tag{3.13}$$

where $|i'\rangle_{\rm out}$ corresponds the collapsed state from $|i\rangle_{\rm out}$.

Now, let us think about the situation in which the observers A and B meet together eventually. The quantum state evolves

$$|\psi\rangle = \frac{1}{\sqrt{N}} \sum_i |i\rangle_{\rm in} |i\rangle_{\rm out} \to \frac{1}{\sqrt{N}} \sum_i a^{(i)}_{i'} |i\rangle_{\rm in} |i'\rangle_{\rm out}. \tag{3.14}$$

Of course, this evolution is not unitary, and the new quantum state does not guarantee the maximum entanglement between two particles.

The paradoxical situation happens because we assumed semi-classical observers A and B. The tunneling process outside corresponds to branching out different histories with different durations of proper time, while the inside exists only one proper time history. If we do not assume the semi-classical observer, then there might be no inconsistency. This again suggests that as long as we are semi-classical observers outside the horizon, the existence of an effective classical spacetime inside the apparent horizons is problematic in the firework model. However, one can still ask why we cannot consider such a semi-classical observer; otherwise, if we assume such a semi-classical observer, does the firework model indicate the loss of information? The real answer to the question is beyond the scope of the present paper, but our construction strongly suggests a critical question for the consistency of the firework model.

4 Discussion

In this paper, we revisited some aspects of the black hole fireworks (i.e. a black hole to white hole transition) scenario proposed in [1, 25]. We constructed an explicit model for the black hole fireworks using the cut-and-paste technique. First, we used the evolution of a time-like shell in the background of the loop quantum gravity inspired metric to model the process of gravitational collapse. Then using the space-like shell analysis, we constructed the firework geometry. We used well-defined thin-shell techniques where all the relevant quantities are clearly defined. Thus, our analysis removes some subtle issues that were present in the previous literature.

We showed that the firework scenario requires specific conditions outside the event horizon, in principle the violation of the energy conditions. This can be expressed in terms of the tension of the space-like junction where the two metrics meet. In particular, we used a rather simple and well-studied space-like junction technique to create the black-to-white hole bounce with a single asymptotic region. For comparison, in ref. [1], a more complicated cut-and-paste procedure is utilized to achieve the same goal without violating the null energy condition far away from the horizon. However, such a cut corresponds to a hypersurface that changes its characteristic from spacelike to null, and thus, corners exist outside of the outer event horizon. The tension conditions for such a scenario are highly non-trivial and might not be physically justifiable. We leave this issue for future work.

Apart from the issue of the junction condition mentioned above, we point out a more fundamental issue related to the black hole firework scenarios in general. Such an issue exists both in the spacetime constructed here and in the original work [1], regardless of whether Israel junction conditions are strictly followed or not. Namely, due to the required cut-and-paste procedure aiming to obtain a spacetime with a single asymptotic region, the bouncing time interval defined by a distant observer suffers from the arbitrariness of the spacelike cut that one is free to choose. In contrast, this arbitrariness has little effect on the infalling observer in our model and, furthermore, has zero effect on the infalling observer living in the spacetime given in ref. [1]. We further argue that from the physical point of view, this arbitrariness for the distant observer cannot be removed. In contrast, as long as there exists an effective classical spacetime inside the event horizon, the bouncing time interval defined by the infalling observer does not have similar randomness. If accumulated quantum gravity effects outside of the horizon drive the bounce (as argued in ref. [1]) and indeed cause the randomness in the duration of the bounce, then the assumption of an effectively classical spacetime inside the inner horizons in the firework scenario might not be justified. Our conclusion is aligned with the quantum-mechanical formation and evaporation of a black hole described in [35]; see figure 5 therein.

At the end, we note that many other questions still remain. How can we justify all the assumptions and calculations in a rigorous framework of quantum gravity? Will the possibility of choosing the time slices arbitrarily still be valid in an evaporating black hole background? We leave these interesting topics for future work.

JCAP01(2025)098

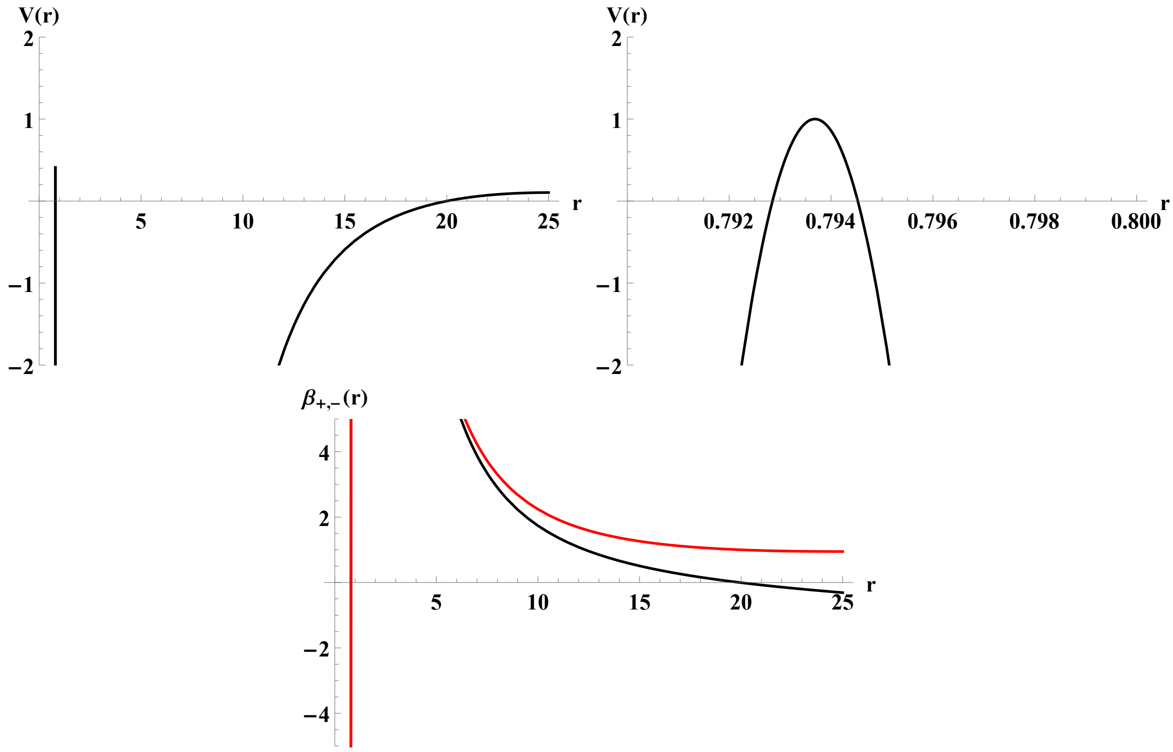

Figure 7. Dynamics of the time-like shell. Top left: $V_{\rm eff}$ with $M = 10$, $A = 0.1$, and $\sigma_0 = 0.04$. There are two bouncing points located at $r_{\rm max} \simeq 19.9993$ and $r_{\rm min} \simeq 0.795$. Note that the outer horizon is $r_+ = 19.9987$ and the inner horizon is $r_- = 0.8046$. Top right: $V_{\rm eff}$ around $r_{\rm min} \simeq 0.795$. Bottom: β_+ (black) and β_- (red). This shows that for $r_{\rm min} \leq r \leq r_{\rm max}$, $\beta_\pm > 0$ conditions are satisfied.

Acknowledgments

DY and WL were supported by the National Research Foundation of Korea (Grant No.: 2021R1C1C1008622, 2021R1A4A5031460). DS is partially supported by the US National Science Foundation, under Grants No. PHY-2014021 and PHY-2310363.

A The junction equations and solutions

A.1 Numerical results for the time-like shell

Figure 7 is an example that describes the gravitational collapse of a time-like shell and the formation of a black hole. Top left and right of figure 7 are $V_{\rm eff}$, where we choose $M = 10$, $A = 0.1$, and $\sigma_0 = 0.04$. For these values of parameters, $r_+ = 19.9987$ and $r_- = 0.8046$. By evaluating $V_{\rm eff}$, we find two bouncing points $r_{\rm max} \simeq 19.9993$ and $r_{\rm min} \simeq 0.795$. Therefore, $r_{\rm min} < r_-$ and $r_{\rm max} > r_+$, and hence, the shell propagates from the region outside of the outer horizon to the region inside of the inner horizon. In addition, bottom of figure 7 shows β_+ (black) and β_- (red), which indicates that for a classically allowed region $r_{\rm min} \leq r \leq r_{\rm max}$, the extrinsic curvatures $\beta_\pm$ are always positive, as we expected.

If we summarize these numerical results, one can conceptually reconstruct figure 2 as a Penrose diagram. The time-like shell is located between $r_{\rm min} \leq r \leq r_{\rm max}$, where $r_{\rm max}$

JCAP01(2025)098

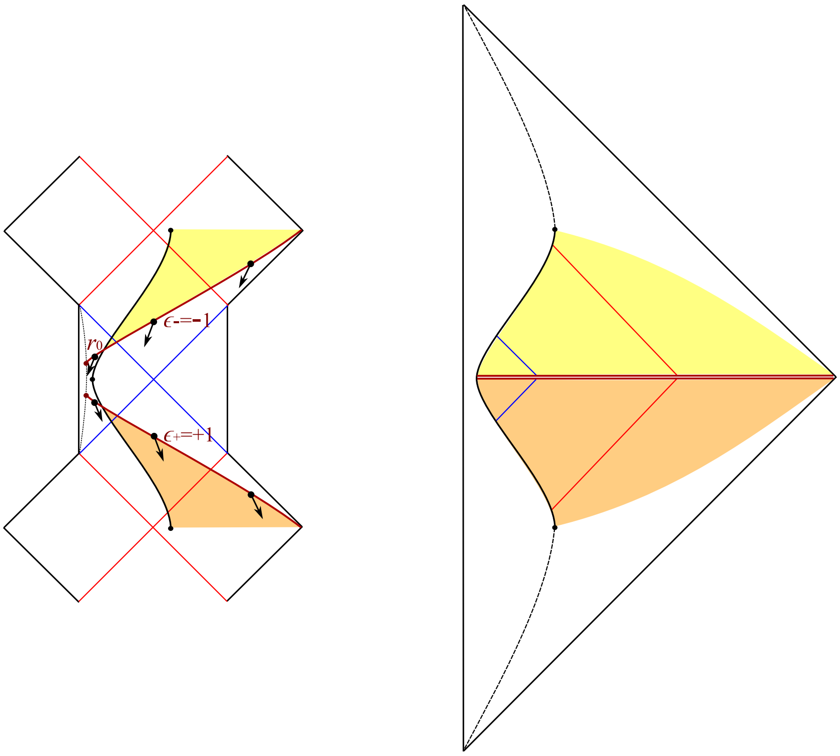

Figure 8. Left: the space-likes shells with $\epsilon_- = -1$ (upper) and $\epsilon_+ = +1$ (lower), where small black arrows denote the outward normal direction. We paste the future of the upper shell ($\tilde{f}_-$, yellow-colored region) and the past of the lower shell ($\tilde{f}_+$, orange-colored region). Right: after we paste two regions, we obtain the final causal structure of the black hole fireworks.

is outside the outer horizon and $r_{\rm min}$ is inside the inner horizon. Using the cut-and-paste technique, we paste a Minkowski space inside the shell. On the right side of the figure 2, there are dashed curves. These curves apparently do not follow the thin-shell trajectories. However, assuming some properties of a star interior, it is reasonable to assume that such a stationary shell is located outside the horizon [33].

A.2 Space-like thin-shells and black hole fireworks

To consider the black hole firework scenario, we need to cut and paste on top of figure 2. We introduce a space-like shell and use it to paste two space-like slices [28]. (All the slices we have implemented on the black hole solution described by the metric (2.2) are shown in figure 8 (left).)

The metric outside and inside the shell:

$$ds^2_\pm = -\frac{1}{\tilde{f}_\pm(r)}dr^2 + \tilde{f}_\pm(r)dt^2 + r^2 d\Omega^2, \tag{A.1}$$

where $+$ and $-$ denote outside and inside the shell. The metric of the space-like shell is

$$ds^2_{\rm shell} = ds^2 + r^2(s)d\Omega^2. \tag{A.2}$$

JCAP01(2025)098

Here, we impose that

$$\tilde{f}_{\pm}(r) = -f(r) = -1 + \frac{2M}{r} - \frac{AM^2}{r^4}, \tag{A.3}$$

in other words, the regions outside and inside the shell correspond to the black hole solution in question.

After imposing the junction equation [34], the result is

$$\epsilon_{-}\sqrt{\dot{r}^2 + \tilde{f}_{-}} - \epsilon_{+}\sqrt{\dot{r}^2 + \tilde{f}_{+}} = 4\pi r\sigma(r), \tag{A.4}$$

where $\sigma(r)$ is the tension of the shell, and $\epsilon_{\pm} = \pm 1$ are the signs of the extrinsic curvatures. Here, the extrinsic curvatures $\tilde{\beta}_{\pm}$ are

$$\tilde{\beta}_{\pm} \equiv \frac{\tilde{f}_{-} - \tilde{f}_{+} \mp 16\pi^2\sigma^2 r^2}{8\pi\sigma r} = \epsilon_{\pm}\sqrt{\dot{r}^2 + \tilde{f}_{\pm}}. \tag{A.5}$$

Note that if $\epsilon_{\pm} = +1$, r increases along the outward normal direction (direction from future to the past), while if $\epsilon_{\pm} = -1$, r decreases along the outward normal direction. Therefore, in our case, we assume that $\epsilon_{+} = +1$ and $\epsilon_{-} = -1$. Hence, $\sigma < 0$ is required, and the null energy condition must be violated. This is expected because of the repulsive term in eq. (2.2).

After simple computations, we obtain the equation

$$\dot{r}^2 + \tilde{V}_{\text{eff}}(r) = 0, \tag{A.6}$$

where

$$\tilde{V}_{\text{eff}}(r) = \tilde{f}_{+} - \frac{\left(\tilde{f}_{-} - \tilde{f}_{+} - 16\pi^2\sigma^2 r^2\right)^2}{64\pi^2\sigma^2 r^2}. \tag{A.7}$$

We now need to assume the condition for the thin-shell. The energy conservation equation is

$$\dot{\sigma} = -2\frac{\dot{r}}{r}\left(\sigma - \lambda\right), \tag{A.8}$$

where λ is the pressure of the shell. If we assume the equation of state of the space-like shell $w_i = -\lambda_i/\sigma_i$ to be a constant, the generic solution of this equation is

$$\sigma(r) = \sum_i \frac{\sigma_{0i}}{r^{2(1+w_i)}}, \tag{A.9}$$

where σ_{0i} are constants.

By assuming a specific function of the tension, we want to impose the following conditions:

- 1. The shell covers the region from $r_0 < r_{\min}$ to infinity, i.e., $\tilde{V}(r) < 0$ for $r_0 \leq r \leq \infty$.
- 2. Extrinsic curvatures satisfy $\tilde{\beta}_{+} > 0$ and $\tilde{\beta}_{-} < 0$ for $r_{\min} \leq r \leq \infty$.

In order to satisfy the extrinsic curvature conditions, the null energy condition of the shell must be violated. For example, figure 9 shows the case when the shell has a constant negative tension (a domain wall case). Figure 10 shows the case where the tension asymptotically

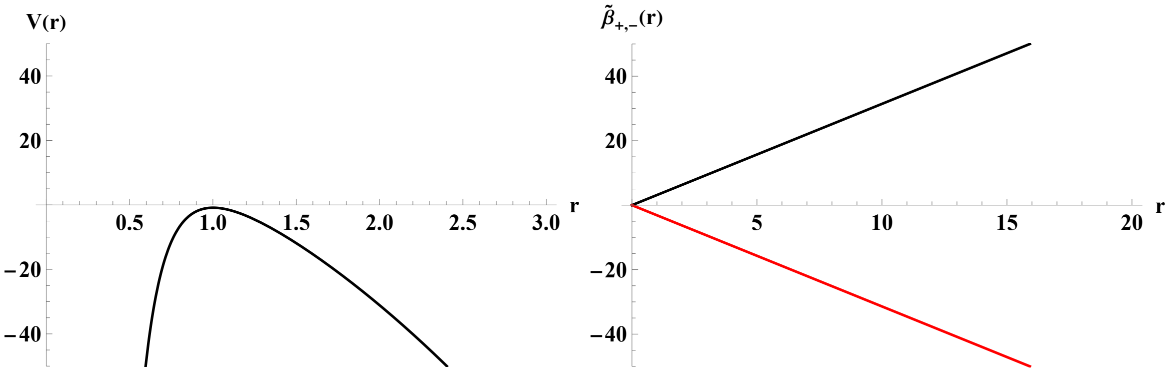

Figure 9. Dynamics of a space-like shell. Left: V_{eff} with $M = 10$, $A = 0.1$, $\sigma_0 = -0.5$, and $w = -1$. This shows that the space-like shell covers the space from infinity to the center. Right: $\tilde{\beta}_+$ (black) and $\tilde{\beta}_-$ (red). This shows that $\tilde{\beta}_+ > 0$ and $\tilde{\beta}_- < 0$ as expected.

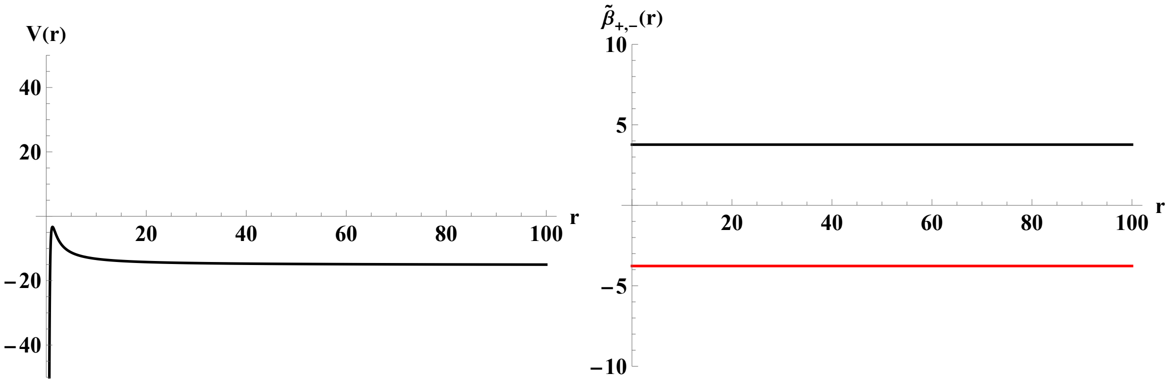

Figure 10. Another example of a space-like shell. Left: V_{eff} with $M = 10$, $A = 0.1$, $\sigma_0 = -0.6$, and $w = -0.5$. Again, the space-like shell covers the region from infinity to the center. Right: $\tilde{\beta}_+$ (black) and $\tilde{\beta}_-$ (red). This shows that $\tilde{\beta}_+ > 0$ and $\tilde{\beta}_- < 0$ as expected.

approaches zero at infinity ($w = -0.5$ and $\sigma \sim 1/r$), and thus the negative tension effects disappear at infinity.

After we cut and paste the spacetimes outside and inside the shell, we obtain the causal structure in figure 8. Outside the shell satisfies $\epsilon_- = -1$, while inside the shell satisfies $\epsilon_+ = +1$. We paste the future of the outer shell (yellow-colored region) and the past of the inner shell (orange-colored region). As a result, we obtain the final causal structure of the black hole fireworks (right of figure 8).

References

[1] M. Han, C. Rovelli and F. Soltani, *Geometry of the black-to-white hole transition within a single asymptotic region*, *Phys. Rev. D* **107** (2023) 064011 [arXiv:2302.03872] [INSPIRE].

[2] S.W. Hawking, *Breakdown of predictability in gravitational collapse*, *Phys. Rev. D* **14** (1976) 2460 [INSPIRE].

[3] D.-H. Yeom and H. Zoe, *Semi-classical black holes with large N re-scaling and information loss problem*, *Int. J. Mod. Phys. A* **26** (2011) 3287 [arXiv:0907.0677] [INSPIRE].

[4] M. Bouhmadi-López et al., *Annihilation-to-nothing: a quantum gravitational boundary condition for the Schwarzschild black hole*, *JCAP* **11** (2020) 002 [arXiv:1911.02129] [INSPIRE].

[5] A. Bogojevic and D. Stojkovic, *A nonsingular black hole*, *Phys. Rev. D* **61** (2000) 084011 [gr-qc/9804070] [INSPIRE].

[6] B.S. DeWitt, *Quantum theory of gravity. 1. The canonical theory*, *Phys. Rev.* **160** (1967) 1113 [INSPIRE].

[7] S. Brahma, C.-Y. Chen and D.-H. Yeom, *Annihilation-to-nothing: DeWitt boundary condition inside a black hole*, *Eur. Phys. J. C* **82** (2022) 772 [arXiv:2108.05330] [INSPIRE].

[8] A. Saini and D. Stojkovic, *Nonlocal (but also nonsingular) physics at the last stages of gravitational collapse*, *Phys. Rev. D* **89** (2014) 044003 [arXiv:1401.6182] [INSPIRE].

[9] E. Greenwood and D. Stojkovic, *Quantum gravitational collapse: non-singularity and non-locality*, *JHEP* **06** (2008) 042 [arXiv:0802.4087] [INSPIRE].

[10] J.E. Wang, E. Greenwood and D. Stojkovic, *Schrodinger formalism, black hole horizons and singularity behavior*, *Phys. Rev. D* **80** (2009) 124027 [arXiv:0906.3250] [INSPIRE].

[11] T. Vachaspati and D. Stojkovic, *Quantum radiation from quantum gravitational collapse*, *Phys. Lett. B* **663** (2008) 107 [gr-qc/0701096] [INSPIRE].

[12] E. Ayon-Beato and A. Garcia, *New regular black hole solution from nonlinear electrodynamics*, *Phys. Lett. B* **464** (1999) 25 [hep-th/9911174] [INSPIRE].

[13] P. Nicolini, A. Smailagic and E. Spallucci, *Noncommutative geometry inspired Schwarzschild black hole*, *Phys. Lett. B* **632** (2006) 547 [gr-qc/0510112] [INSPIRE].

[14] V.P. Frolov, M.A. Markov and V.F. Mukhanov, *Black holes as possible sources of closed and semiclosed worlds*, *Phys. Rev. D* **41** (1990) 383 [INSPIRE].

[15] D.-H. Yeom and H. Zoe, *Constructing a counterexample to the black hole complementarity*, *Phys. Rev. D* **78** (2008) 104008 [arXiv:0802.1625] [INSPIRE].

[16] M. Bouhmadi-López et al., *Traversable wormhole in Einstein 3-form theory with self-interacting potential*, *JCAP* **10** (2021) 059 [arXiv:2108.07302] [INSPIRE].

[17] M. Bojowald, S. Brahma and D.-H. Yeom, *Effective line elements and black-hole models in canonical loop quantum gravity*, *Phys. Rev. D* **98** (2018) 046015 [arXiv:1803.01119] [INSPIRE].

[18] A. Ashtekar, J. Olmedo and P. Singh, *Quantum transfiguration of Kruskal black holes*, *Phys. Rev. Lett.* **121** (2018) 241301 [arXiv:1806.00648] [INSPIRE].

[19] A. Ashtekar, J. Olmedo and P. Singh, *Quantum extension of the Kruskal spacetime*, *Phys. Rev. D* **98** (2018) 126003 [arXiv:1806.02406] [INSPIRE].

[20] C. Barceló, R. Carballo-Rubio and L.J. Garay, *Mutiny at the white-hole district*, *Int. J. Mod. Phys. D* **23** (2014) 1442022 [arXiv:1407.1391] [INSPIRE].

[21] C. Barcelo, R. Carballo-Rubio, L.J. Garay and G. Jannes, *The lifetime problem of evaporating black holes: mutiny or resignation*, *Class. Quant. Grav.* **32** (2015) 035012 [arXiv:1409.1501] [INSPIRE].

[22] M. Bouhmadi-López et al., *Asymptotic non-flatness of an effective black hole model based on loop quantum gravity*, *Phys. Dark Univ.* **30** (2020) 100701 [arXiv:1902.07874] [INSPIRE].

[23] D.K. Hong, W.-C. Lin and D.-H. Yeom, *Trouble with geodesics in black-to-white hole bouncing scenarios*, *Phys. Rev. D* **106** (2022) 104011 [arXiv:2207.03183] [INSPIRE].

[24] A. Ashtekar and M. Bojowald, *Black hole evaporation: a paradigm*, Class. Quant. Grav. **22** (2005) 3349 [gr-qc/0504029] [INSPIRE].

[25] H.M. Haggard and C. Rovelli, *Quantum-gravity effects outside the horizon spark black to white hole tunneling*, Phys. Rev. D **92** (2015) 104020 [arXiv:1407.0989] [INSPIRE].

[26] W. Israel, *Singular hypersurfaces and thin shells in general relativity*, Nuovo Cim. B **44S10** (1966) 1 [*Erratum ibid.* **48** (1967) 463] [INSPIRE].

[27] C. Barceló, R. Carballo-Rubio and L.J. Garay, *Where does the physics of extreme gravitational collapse reside?*, Universe **2** (2016) 7 [arXiv:1510.04957] [INSPIRE].

[28] S. Brahma and D.-H. Yeom, *Effective black-to-white hole bounces: the cost of surgery*, Class. Quant. Grav. **35** (2018) 205007 [arXiv:1804.02821] [INSPIRE].

[29] R. Gaur and M. Visser, *Black holes, white holes, and near-horizon physics*, JHEP **05** (2024) 172 [arXiv:2304.10692] [INSPIRE].

[30] H. Maeda, *Energy conditions for non-timelike thin shells*, Class. Quant. Grav. **40** (2023) 195009 [arXiv:2306.07326] [INSPIRE].

[31] S.K. Blau, E.I. Guendelman and A.H. Guth, *The dynamics of false vacuum bubbles*, Phys. Rev. D **35** (1987) 1747 [INSPIRE].

[32] J.P.W. Taylor, *Junction conditions at a corner*, Class. Quant. Grav. **21** (2004) 3705.

[33] P. Chen, G. Domènech, M. Sasaki and D.-H. Yeom, *Stationary bubbles and their tunneling channels toward trivial geometry*, JCAP **04** (2016) 013 [arXiv:1512.00565] [INSPIRE].

[34] R. Balbinot and E. Poisson, *Stability of the Schwarzschild-de Sitter model*, Phys. Rev. D **41** (1990) 395 [INSPIRE].

[35] J. Hartle and T. Hertog, *Quantum transitions between classical histories*, Phys. Rev. D **92** (2015) 063509 [arXiv:1502.06770] [INSPIRE].

JCAP01(2025)098